

The Density Functional Tight Binding (DFTB) Approach for Investigating Vacancy and Doping in Graphene as Hydrogen Storage

Yuniawan hidayat*, Fitria Rahmawati, Khoirina Dwi Nugrahaningtyas, Paulus Bagus Swandito
Chemistry Department, Faculty of Mathematics and Natural Sciences, Sebelas Maret University, Surakarta, Indonesia

Corresponding Author:
Yuniawan Hidayat
yuniawan.hidayat@staff.uns.ac.id

Received: October 2023
Accepted: December 2023
Published: March 2024

©Yuniawan Hidayat et al. This is an open-access article distributed under the terms of the Creative Commons Attribution License, which permits unrestricted use, distribution, and reproduction in any medium, provided the original author and source are credited.

Abstract

A study on graphene defects for hydrogen storage has been successfully conducted using the Density Functional Tight Binding (DFTB) approach. The research aimed to modify solid materials for hydrogen storage. A $4 \times 4 \times 1$ unit cell was used as the basis, while the supercell used for sampling was enlarged to $40 \times 40 \times 1$. The analyzed data included changes in Density of States (DOS), Fermi level shifts, electronic band structures, formation energy, adsorption energy, and isosurfaces for each graphene orientation. It has been observed that modifying the surface structure of graphene can alter the electronic properties of graphene. This is indicated by shifts in DOS intensity, characterized by increased electronic intensity around the Fermi level total density charge different. The interaction energy between graphene and hydrogen gas has been determined to be -0.0155 eV for H-epoxy graphene, -0.4941 eV for H-monovacancy graphene, and -0.0424 eV for HN-monovacancy graphene. The presence of the vacancy increase the potential to adsorb hydrogen.

Keywords: *DFTB, graphene, graphene defects, hydrogen gas, hydrogen storage.*

Introduction

Currently, there are several methods of hydrogen storage, including compressed gas, liquefaction, and adsorption, each with its own advantages and disadvantages. Solid-state hydrogen storage has the potential for high energy density and low weight, but so far, no commercial solution has been found. Therefore, the biggest challenge lies in discovering an effective way to store and transport hydrogen. [1],[2].

CNT and graphene nanoflakes theoretically possess high hydrogen storage capacities [3]-[6]. The presence of alkali metals on the graphene surface can enhance hydrogen storage

capabilities by creating additional surface sites for hydrogen adsorption [7],[8]. Researchers have employed a combination of high temperature and chemical vapor deposition to create graphene with controlled vacancy density, resulting in an increased hydrogen storage capacity compared to pure graphene [9],[10].

Modified graphene exhibits distinct properties compared to pure graphene. The active regions of modified graphene can shift the Fermi level above the Dirac point and alter the Density of States (DOS) near the Fermi level, leading to the formation of a bandgap between the conduction and valence bands [11]-[14]. This bandgap phenomenon is critical as it influences

the interaction between graphene and adsorbed molecules. In general, materials with wider bandgaps tend to have weaker adsorption interactions with other molecules, while those with narrower bandgaps tend to exhibit stronger adsorption interactions [15],[16]. When hydrogen is excessively adsorbed onto graphene, it becomes challenging to release as an energy source, and when adsorption is too weak, its capacity as a hydrogen carrier diminishes. The magnitude of the bandgap in graphene can be finely tuned through modifications involving vacancies, doping, and the introduction of alkali metals such as potassium.

The relationship between the influence of graphene structure, its electronic properties, and the strength of hydrogen gas adsorption needs to be comprehended at the molecular level. Quantum calculation methods are at the forefront in addressing this issue. However, to compute large-scale systems involving thousands of atoms, faster methods are required without compromising accuracy. In a periodic system, a layer of graphene comprises large carbon atoms, making it challenging for DFT and ab initio methods to handle calculations involving hundreds of atoms. Here, we showcase the validity, speed, and reliability of the DFTB method in modeling supercell graphene while evaluating their electronic properties during hydrogen adsorption. Concurrently, we're investigating modified graphene featuring vacancies, epoxy groups, and nitrogen-doped vacancy graphene to refine these characteristics and assess its capacity for attracting hydrogen.

Experimental

Methods

The crystal structure of graphene refers to Kristin Persson's work[17]. The unit cell structure of graphene is constructed from the crystal unit cell of graphite with the following parameters: lattice parameters a , b , and c are 2.468 Å, 2.468 Å, and 8.685 Å, respectively. The lattice angles α , β , and γ are 90°, 90°, and 120°, respectively.

The lattice coordinates for the four carbon atoms are as follows: 0, 0, $\frac{3}{4}$; 0, 0, $\frac{1}{4}$; $\frac{1}{3}$, $\frac{2}{3}$, $\frac{3}{4}$; and $\frac{2}{3}$, $\frac{1}{3}$, $\frac{1}{4}$. The crystal system adheres to a hexagonal structure with a point group of 6/mmm.

To produce graphene layers, the original graphite unit cell is enlarged to a $4 \times 4 \times 1$ unit cell using the VESTA software [18]. The procedure for creating vacancy and N-doped modified graphene follows the approach outlined by Hidayat et al. [19],[20]. The addition of oxygen atoms on top of two carbon atoms in the center of the cell transforms pristine graphene into an epoxy graphene model. In the geometry optimization calculations, the unit cell was expanded into a supercell with dimensions of $40 \times 40 \times 1$. The optimization calculations were conducted with the application of Periodic Boundary Conditions (PBC) using the Self-Consistent Charges-Density Functional Tight Binding (SCC-DFTB) method.

The Slater-Koster mio parameters were employed as DFTB parameters for interatomic interactions. The Fermi smearing method at a temperature near 0 K was employed to generate conserved orbital functions. The k-points in the Brillouin zone were set at Γ (0,0 0,0 0,0), M (0,5 0,0 0,0), and K (0,3333 0,333 0,0). Subsequently, the supercell was optimized until convergence was achieved. The calculation was performed by the DFTB+ software[21].

Modeling the adsorption of hydrogen gas is carried out by positioning hydrogen molecules above the centers of all optimized graphene sheets. The hydrogen molecules are vertically oriented, directing the hydrogen atoms towards the vacancy and doping sites of the graphene. The optimization procedure was then repeated.

The optimized-state calculations provided data on the density of states (DOS), Fermi level, atomic charges, and band energy structure for each model. The calculation of these electronic parameters depends on the geometry of the modeled system. The modeled system is

considered ideal when it possesses the lowest energy and its values align with a valid reference. Subsequently, the DOS graph and band structure were adjusted to align with a Fermi level of 0 eV, as determined by $E_0 - E_f$. E_0 represents the reference Fermi level set at 0 eV, while E_f denotes the calculated Fermi level.

The formation energy of the GO surface containing either "n" epoxy groups denoted as E_f , is calculated using equation 1 [20]

$$E_f = E_{GO} - E_{PG} - nE_O \quad (1)$$

Where E_{GO} , E_{PG} , and nE_O represent the total energy of the graphene with epoxy group, pure graphene, and the number of free epoxy groups (O atoms), respectively. The energy E_O is obtained by optimizing O_2 using the same optimization procedure, with the resulting energy divided by two.

The formation energy of nitrogen-modified monovacancy graphene can be calculated using the equation 2

$$E_f = E_{tot} - n_N E_N + n_C E_C - E_{PG} \quad (2)$$

Here, E_{tot} represents the total energy of the modified graphene with vacancies or doping.

The variables n_N and E_N correspond to the number of atoms and the energy of the N-dopant, while n_C and E_C refer to the number of removed carbon atoms and its energy. Lastly, the E_{PG} represents the total energy of pristine, unmodified graphene.

The interaction energy of hydrogen adsorption on the graphene surface, in terms of adsorption energy (E_{ads}), is calculated using the equation 3

$$E_{ads} = E_{complex} - (E_{GM} + E_{Hydrogen}) \quad (3)$$

In this equation, $E_{complex}$ represents the energy of the hydrogen model adsorbed on the modified graphene surface, E_{GM} is the energy of the modified graphene, and $E_{Hydrogen}$ is the energy of the H_2 .

Results and Discussion

The optimization of graphene's structure was performed using the DFTB (Density Functional Tight Binding) method within its crystal lattice vectors x , y , and z . In the accompanying image, carbon atoms are depicted in brown, oxygen atoms in red, nitrogen atoms in silver, and hydrogen atoms in white. The optimization results for graphene are visualized in the Figure 1.

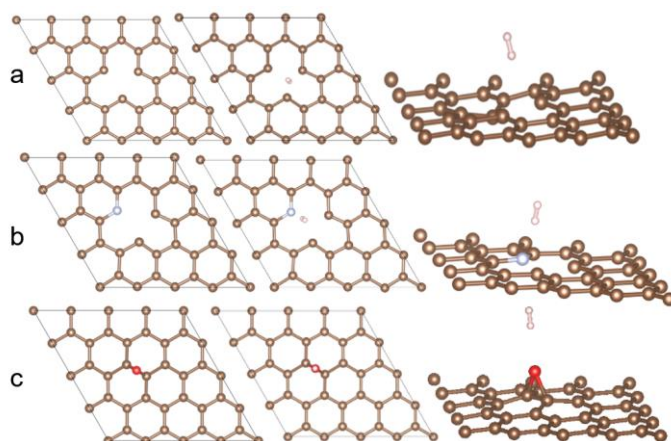


Figure 1. Visualization of optimized graphenes without and with adsorbed hydrogen (a) Vacany graphehene (b) N-doped vacancy graphene and (c) Epoxy fungtionalized graphene. Brown, cyan, red and with refer to C, N, O and H, respectively.

The geometry optimization for monovacancy graphene reveals C-C bond distances ranging from 1.4142 to 1.4603 Å. However, based on XRD, EXAFS, and EDX analyses, pristine graphene exhibits highly symmetrical single distances at 1.42 Å [22]-[24]. This confirms that the symmetry is reduced around the vacancy site. The presence of Hydrogen change influences the C-C distance of the graphene ranging from 1.4045 to 1.4596 Å, and the H₂ molecule closed to one of the carbon atoms (C-H) in the vacancy site at a distance of 2.3816 Å.

In monovacancy N-graphene, the carbon-carbon (C-C) bond distance falls within the range of 1.4137 to 1.5128 Å, while the nitrogen-carbon (N-C) bond distance is approximately 1.3413 Å. These findings closely concistence with data obtained through Density Functional Theory (DFT) calculations, which typically predict C-C bond distances in the range of approximately 1.41 to 1.45 Å [25],[26]. On the other hand, in the presesnce of H₂, the C-C bond distance ranges from 1.4139 to 1.5127 Å, and the C-N bond distance is around 1.3411 Å. These results suggest that there is no significant effect on the graphene structure when hydrogen (H₂) is adsorbed.

The optimization results for epoxy graphene show that the distance between carbon atoms (C-C) ranges from 1.4140 to 1.5135 Å, while the distance between carbon and oxygen atoms (C-O) ranges from 1.4964 to 1.4965 Å. For hydrogen-functionalized graphene epoxy, the C-C distance ranges from 1.4139 to 1.5129 Å, and the C-O distance ranges from 1.4979 to 1.4980 Å. The presence of hydrogen on the surface did not significantly influence the

structure of graphene. The distance was found to be equal using both the ab initio and DFT methods [27][28][29]. Additionally, the distance between H₂ atoms is 0.7451 Å, and the closest distance between an H atom and an O atom is 2.235 Å.

Based on the calculations, it was found that epoxy graphene has a formation energy of -3.3721 eV. These results align with the research conducted by Prasert and Sutthubutpong using the DFT method, which reported a formation energy for epoxy graphene ranging from -3.092 eV to -3.231 eV [30]. Meanwhile, for monovacancies, the DFTB method yielded a formation energy of 8.2594 eV, which is in close agreement with previous research by Ali and colleagues, who used the DFT method and reported values between 7.19 and 7.78 eV [31]. In the case of N-graphene monovacancies, the obtained formation energy is 5.9785 eV. Positive formation energy values indicate thermodynamic instability. The formation energy values for all three types of graphene are consistent with the DFT calculation method. Table 1 show in details the formation energi with other methods.

Figure 2 shows all comparison of DOS graphene before and after adsorb hydrogen. The fermi level has been shift to the refence point (0). Based on the graph, it is evident that the interaction between epoxy graphene and hydrogen gas does not significantly alter the DOS spectra. There is only a minor increase in electronic intensity within the valence band region at approximately -4 eV to -3 eV (Figure 2a).

Table 1. Formation energy and fermi level of modeled grafena

Struktur	Metode	Ef (eV)	Fermi Level (eV)	Ref
Epoxy graphene	DFTB	-3.3721	-4.8243	This work [30]
	DFT	-3.231		
Monovacancy graphene	DFTB	8.2594	-4.7329	This work [31]
	DFT	7.78		
N-monovacancy graphene	DFTB	5.978	-4.9001	THis work [25] [26] [32]
	DFT	4.31	-	
	DFT	5.93	-	
N-graphene	CVD	-	-4.5	

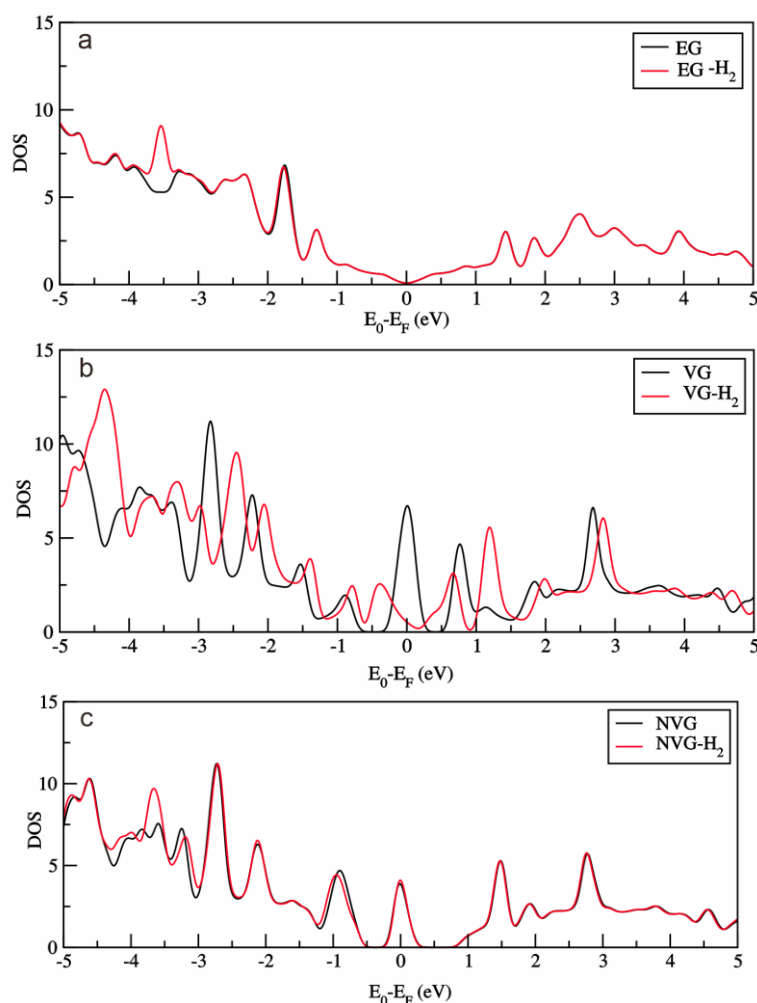


Figure 2. DOS comparison before and after adsorb Hydrogen (a) Epoxy graphene (EG) (b) Monovacancy graphene (VG) (c) N-monovacancy graphene (NVG)

Table 2. Interaction energy modeled graphenes with H₂

Graphene	Method	E _{ads} (eV)	Reference
Epoxy graphene	DFTB	-0.0155	This work
Monovacancy graphene	DFTB	-0.4941	This work
N-monovacancy graphene	DFT	-0.3282 - 0.402	[9]
	DFTB	-0.0424	This work
	DFT	-0.04	[10]
	DFT	-0.059	[11]

The interaction between hydrogen gas and monovacancy graphene indeed alters the Density of States (DOS) spectra precisely at the Dirac point in the Fermi level region. This is because hydrogen adsorbs at the vacancy site, leading to an increase in intensity at that specific point (Figure 2b). The interaction between hydrogen gas and N-graphene

monovacancy does not significantly alter the Density of States (DOS) spectra. There is a minor increase in electronic intensity primarily within its conduction band region at approximately -4.5 eV to -3 eV, with only minimal changes observed in the rest of the conduction band (figure 2c).

Table 2 displays the hydrogen adsorption energies on graphene. Based on the calculations, the interaction energy for H-epoxy graphene is -0.0155 eV, for H-monovacancy graphene it is -0.0424 eV, and for H-N-monovacancy graphene it is -0.4941 eV. The DFT method yielded hydrogen adsorption energies on monovacancy graphene ranging from -0.3282 eV to -0.402 eV [9]. This indicates that the DFTB method demonstrates good validity for modeling H₂ gas adsorption on various graphene models. Additionally, graphene monovacancy doped with N shows adsorption capabilities equivalent to potassium-doped graphene (-0.04 eV)^[10]. Other research reports that N-doped graphene can adsorb hydrogen with an energy of -0.059 eV^[11]. Here the adsorption hydrogen tend to follow physisorption mechanism.

The potential energy interaction scan of H₂ with graphene was conducted to observe the equilibrium bond distance between H₂ and graphene. It's important to note that the distance of H₂ on graphene with vacancies is calculated from the midpoint of the vacancy surface, and this distance varies vertically. With the exception of epoxy graphene, the varied H₂ distance is measured from the epoxy. The

potential energy scan between H₂ and modeled graphene, as a function of distance, is depicted in Figure 3. Sequentially, the closest distances between hydrogen and the graphene surface are as follows: in monovacancy graphene (2.0 Å), nitrogen-doped monovacancy graphene (2.0 Å), and epoxy graphene (2.2 Å). This sequence arises as a consequence of their adsorption energies. Geometry optimization within the equilibrium distance range resulted in the following interaction distances of H₂ with the nearest atoms: H₂-O on epoxy graphene at 2.23 Å, H₂-N on nitrogen-doped monovacancy graphene at 2.06 Å, and the closest H₂-C on monovacancy graphene at 2.381 Å.

The orientation of hydrogen adsorption on the graphene surface is confirmed by the total charge difference between the graphene surface and hydrogen. Figure 3 shows that hydrogen is adsorbed vertically, with the hydrogen atoms having partial positive charges being directed towards the graphene surface, which has partial negative charges. The highest adsorption energy on graphene monovacancy is due to the presence of two carbon atoms in the vacancy site region with partial negative charges (Figure 3b).

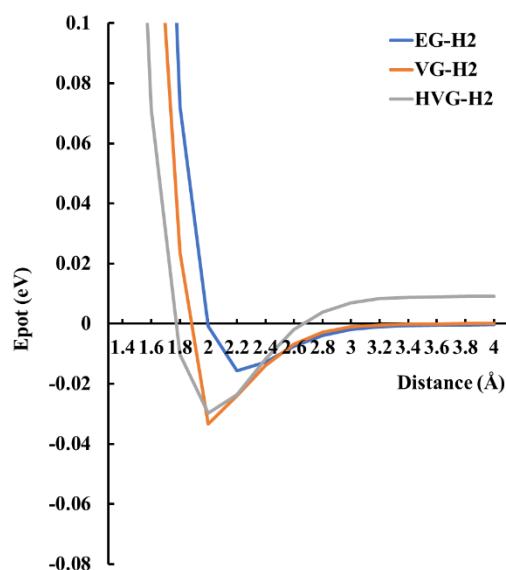


Figure 3. Potential Energy of adsorbed H₂ on the modeled graphenes

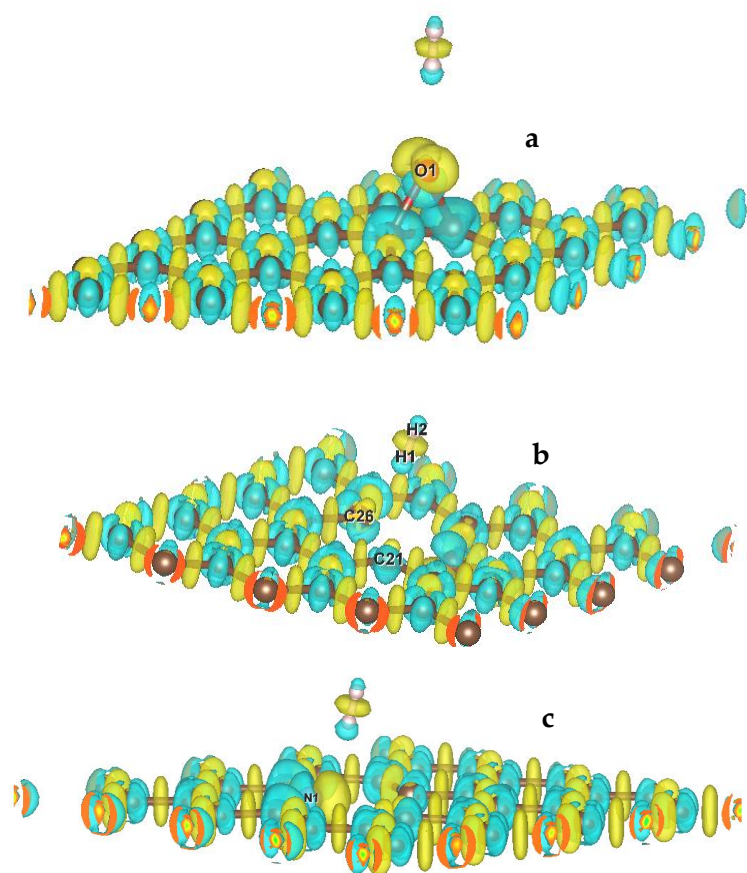


Figure 3. The charge density difference of adsorbed hydrogen on the graphene surface. Yellow represents the negative surface, and cyan represents the positive surface (a) H-epoxy graphene, (b) H-monovacancy graphene (c) HN-Monovacancy graphene

The interaction with N-monovacancy graphene is relatively stronger compared to epoxy, as evident from the larger size of the hydrogen charge density (shown in blue) in Figure 3c and Figure 3a. In general, the presence of vacancies enhances the interaction potential with hydrogen, while epoxy graphene allows hydrogen to move more freely, resulting in lower adsorption energy.

Conclusions

Adsorption of hydrogen on modeled graphene is mainly described as physisorption. The existence of hydrogen gas does not have a significant impact on graphene's electronic properties. This makes sense since weak interactions do not possess the ability to strongly transfer charges. On the other hand,

the presence of vacancies can increase the interaction potential between hydrogen and graphene. The DFTB approach has been successfully employed to explore and elucidate the relationship between the properties of modified graphene in adsorbing H₂.

Acknowledgments

The author expresses gratitude to the Ministry of Research, Technology, and Higher Education for funding this research project through the Fundamental Research Scheme in 2023.

References

1. Demirel, Y., *Green Energy and Technology*. Green Energy and Technology, BENTHAM SCIENCE PUBLISHERS, (2006). doi:10.2174/97816080528511060101

2. Yu, K., Li, J., Qi, H. & Liang, C., High-capacity activated carbon anode material for lithium-ion batteries prepared from rice husk by a facile method. *Diam. Relat. Mater.*, **86**(January): 139–145 (2018).
3. Tachikawa, H. & Iyama, T., Mechanism of Hydrogen Storage in the Graphene Nanoflake–Lithium–H₂ System. *J. Phys. Chem. C*, **123**(14): 8709–8716 (2019).
4. Hosseini, S. V., Arabi, H. & Kompany, A., Silicon atom and silicon oxide molecule, within the metallic and semiconducting carbon nanotubes as promising centers candidates for hydrogen adsorption: A DFT theoretical study. *Int. J. Hydrogen Energy*, **43**(39): 18306–18315 (2018).
5. Briggs, N. M., Barrett, L., Wegener, E. C., Herrera, L. V., Gomez, L. A., Miller, J. T. & Crossley, S. P., Identification of active sites on supported metal catalysts with carbon nanotube hydrogen highways. *Nat. Commun.*, **9**(1): (2018).
6. Ahadi, Z., Shadman, M., Yeganegi, S. & Asgari, F., Hydrogen adsorption capacities of multi-walled boron nitride nanotubes and nanotube arrays: A grand canonical Monte Carlo study. *J. Mol. Model.*, **18**(7): 2981–2991 (2012).
7. Lee, S. H. & Jhi, S. H., A first-principles study of alkali-metal-decorated graphyne as oxygen-tolerant hydrogen storage media. *Carbon N. Y.*, **C**(81): 418–425 (2015).
8. Kaiser, A., Renzler, M., Kranabetter, L., Schwärzler, M., Parajuli, R., Echt, O. & Scheier, P., On enhanced hydrogen adsorption on alkali (cesium) doped C₆₀ and effects of the quantum nature of the H₂ molecule on physisorption energies. *Int. J. Hydrogen Energy*, **42**(5): 3078–3086 (2017).
9. Cui, H., Zhang, Y., Tian, W., Wang, Y., Liu, T., Chen, Y., Shan, P., *et al.*, A study on hydrogen storage performance of Ti decorated vacancies graphene structure on the first principle. *RSC Adv.*, **11**(23): 13912–13918 (2021).
10. Yahya, M. S., Sunnardianto, G. K. & Handayani, M., The effect of single and double vacancy on hydrogenated graphene for hydrogen storage application. *IOP Conf. Ser. Mater. Sci. Eng.*, **541**(1): 012005 (2019).
11. Zhang, L. & Xia, Z., Mechanisms of Oxygen Reduction Reaction on Nitrogen-Doped Graphene for Fuel Cells. *J. Phys. Chem. C*, **115**(22): 11170–11176 (2011).
12. Hidayat, Y., Rahmawati, F., Heraldy, E., Nugrahaningtyas, K. & Nurcahyo, I., The Effect Of Sulphur (S) Doping and K⁺ Adsorption To The Electronic Properties Of Graphene: A Study By DFTB Method. *J. Ris. Kim.*, **13**(2): 130–137 (2022).
13. Ketabi, N., de Boer, T., Karakaya, M., Zhu, J., Podila, R., Rao, A. M., Kurmaev, E. Z., *et al.*, Tuning the electronic structure of graphene through nitrogen doping: experiment and theory. *RSC Adv.*, **6**(61): 56721–56727 (2016).
14. Joucken, F., Tison, Y., Le Fèvre, P., Tejada, A., Taleb-Ibrahimi, A., Conrad, E., Repain, V., *et al.*, Charge transfer and electronic doping in nitrogen-doped graphene. *Sci. Rep.*, **5**(1): 14564 (2015).
15. Maeda, K., Ishimaki, K., Tokunaga, Y., Lu, D. & Eguchi, M., Modification of Wide-Band-Gap Oxide Semiconductors with Cobalt Hydroxide Nanoclusters for Visible-Light Water Oxidation. *Angew. Chemie Int. Ed.*, **55**(29): 8309–8313 (2016).
16. Castelli, I. E., Man, I.-C., Soriga, S.-G., Parvulescu, V., Halck, N. B. & Rossmesl, J., Role of the Band Gap for the Interaction Energy of Coadsorbed Fragments. *J. Phys. Chem. C*, **121**(34): 18608–18614 (2017).
17. Persson, K., Materials Data on C (SG:194) by Materials Project. (2014). doi:10.17188/1208406
18. Momma, K. & Izumi, F., VESTA: a three-dimensional visualization system for electronic and structural analysis. *J. Appl. Crystallogr.*, **41**(3): 653–658 (2008).
19. Hidayat, Y., Rahmawati, F., Nugrahaningtyas, K. D., Althof Abiyyi, A., Erlangga, M. Z. & Pujiastuti, N., Exploring the electronic properties of N-doped graphene on graphitic and pyridinic models and its interaction with K. *Aust. J. Chem.*, **75**(5): 325–330 (2022).

20. Hidayat, Y., Rahmawati, F. & Nugrahaningtyas, K. D., Does Divacancy Defect Combine with N,S-Codoping Enhance the Electronic Properties of Graphene to Its Interaction with K⁺ Ion? *J. Mol.*, **18(1)**: 140–146 (2023).
21. Hourahine, B., Aradi, B., Blum, V., Bonafé, F., Buccheri, A., Camacho, C., Cevallos, C., *et al.*, DFTB+, a software package for efficient approximate density functional theory based atomistic simulations. *J. Chem. Phys.*, **152(12)**: 124101 (2020).
22. Burian, A., Dore, J. C. & Jurkiewicz, K., Structural studies of carbons by neutron and x-ray scattering. *Reports Prog. Phys.*, **82(1)**: 016501 (2018).
23. Buades, B., Moonshiram, D., Sidiropoulos, T. P. H., León, I., Schmidt, P., Pi, I., Di Palo, N., *et al.*, Dispersive soft x-ray absorption fine-structure spectroscopy in graphite with an attosecond pulse. *Optica*, **5(5)**: 502 (2018).
24. Shibazaki, Y., Kono, Y. & Shen, G., Compressed glassy carbon maintaining graphite-like structure with linkage formation between graphene layers. *Sci. Rep.*, **9(1)**: 7531 (2019).
25. Yu, Y. X., Can all nitrogen-doped defects improve the performance of graphene anode materials for lithium-ion batteries? *Phys. Chem. Chem. Phys.*, **15(39)**: 16819–16827 (2013).
26. Yang, M., Wang, L., Li, M., Hou, T. & Li, Y., Structural stability and O₂ dissociation on nitrogen-doped graphene with transition metal atoms embedded: A first-principles study. *AIP Adv.*, **5(6)**: 067136 (2015).
27. Chaban, V. V. & Prezhdo, O. V., Structure and energetics of graphene oxide isomers: ab initio thermodynamic analysis. *Nanoscale*, **7(40)**: 17055–17062 (2015).
28. Prias, J., Mejía Mendoza, L., Velasco, M., Perea, J., Aspuru-Guzik, A., Acosta Minoli, C., Prías-Barragán, J. J., *et al.*, Graphene Oxide: Comparisons between Experimental and Computational Simulation of HR-TEM Images. 0–20 (2022).
29. Thuy Tran, N. T., Lin, S.-Y., Glukhova, O. E. & Lin, M.-F., π -Bonding-dominated energy gaps in graphene oxide. *RSC Adv.*, **6(29)**: 24458–24463 (2016).
30. Prasert, K. & Sutthibutpong, T., Unveiling the Fundamental Mechanisms of Graphene Oxide Selectivity on the Ascorbic Acid, Dopamine, and Uric Acid by Density Functional Theory Calculations and Charge Population Analysis. *Sensors*, **21(8)**: 2773 (2021).
31. Mirzaei, A., Bharath, S. P., Kim, J.-Y., Pawar, K. K., Kim, H. W. & Kim, S. S., N-Doped Graphene and Its Derivatives as Resistive Gas Sensors: An Overview. *Chemosensors*, **11(6)**: 334 (2023).
32. Deokar, G., Jin, J., Schwingenschlögl, U. & Costa, P. M. F. J., Chemical vapor deposition-grown nitrogen-doped graphene's synthesis, characterization and applications. *npj 2D Mater. Appl.* **2022** 61, **6(1)**: 1–17 (2022).